Quantitative Estimates of Cloudiness over the Gulf Stream Locale Using GOES VAS Observations

RANDALL J. ALLISS AND SETHU RAMAN

Department of Marine, Earth and Atmospheric Sciences, North Carolina State University, Raleigh, North Carolina

(Manuscript received 23 December 1993, in final form 18 April 1994)

ABSTRACT

Fields of cloudiness derived from the Geostationary Operational Environmental Satellite VISSR (Visible–Infrared Spin Scan Radiometer) Atmospheric Sounder are analyzed over the Gulf Stream locale (GSL) to investigate seasonal and geographical variations. The GSL in this study is defined as the region bounded from 31° to 38°N and 82° to 66°W. This region covers an area that includes the United States mid-Atlantic coast states, the Gulf Stream, and portions of the Sargasso Sea. Clouds over the GSL are found approximately three-quarters of the time between 1985 and 1993. However, large seasonal variations in the frequency of cloudiness exist. These seasonal variations show a distinct relationship to gradients in sea surface temperature (SST). For example, during winter when large SST gradients are present, large gradients in cloudiness are found. Clouds are observed least often during summer over the ocean portion of the GSL. This minimum coincides with an increase in atmospheric stability due to large-scale subsidence. Cloudiness is also found over the GSL in response to mesoscale convergence areas induced by sea surface temperature gradients. Geographical variations in cloudiness are found to be related to the meteorology of the region. During periods of cold-air advection, which are found most frequently in winter, clouds are found less often between the coastline and the core of the Gulf Stream and more often over the Sargasso Sea. During cyclogenesis, large cloud shields often develop and cover the entire domain.

Satellite estimates of cloudiness are found to be least reliable over land at night during the cold months. In these situations, the cloud retrieval algorithm often mistakes clear sky for low clouds. Satellite-derived cloudiness over land is compared with daytime surface observations of cloudiness. Results indicate that retrieved cloudiness agrees well with surface observations. Relative humidity fields taken from global analyses are compared with satellite cloud heights at three levels in the atmosphere. Cloudiness observed at these levels is found at relative humidities in the 75%–100% range but is also observed at humidities as low as 26%.

1. Introduction

The Atlantic Ocean region along the United States mid-Atlantic coast is often dominated by large sensible and latent heat fluxes. These fluxes are due in part to the presence of the Gulf Stream and its proximity to the east coast of the United States. According to Budyko (1963), the annual heat loss (gain to the atmosphere) by the fast-moving Gulf Stream is greater here than in any other area of any ocean basin. The heat loss from the warm Gulf Stream waters is the result of rapid advection of warm water from the subtropical regions (i.e., the Gulf of Mexico) into an area dominated by relatively cold dry continental air masses. The average annual heat loss from the ocean in this region has been estimated to be greater than 200 W m^{-2} (Bunker 1976). The key to the great heat loss lies in the large dewpoint depression relative to the sea surface temperature (SST). Throughout most of the fall and winter the dewpoint depression exceeds 10 K. This, coupled with winds averaging more than 12 m s^{-1}, produces a latent heat flux (LHF) exceeding 300 W m^{-2} for five months of the year (Bunker 1976). The sensible heat flux (SHF) is also large, except during summer because of the large air–sea temperature difference. These conditions make the Gulf Stream locale (GSL) a preferred area for the production of cloudiness. Clouds over the GSL are also due in part to cyclogenesis or the redevelopment of midlatitude cyclones, cold air outbreak episodes, and convection induced by mesoscale convergence zones that are driven by gradients in SST. All of these processes, however, are driven by surface sensible and latent heat fluxes.

Recently the GSL has been the focus of several field experiments (Genesis of Atlantic Lows Experiment, GALE 1986; Experiment on Rapidly Intensifying Cyclones over the Atlantic, ERICA 1989) designed to investigate various aspects of cyclogenesis, including the structure of the convective marine boundary layer during cold-air outbreaks (Raman et al., 1986; Raman and Riordan 1988; Dirks et al. 1988; Wayland and Raman 1989; Holt and Raman 1990; Vukovich et al. 1991; Huang and Raman 1991; Chang et al. 1993).

Corresponding author address: Dr. Sethu Raman, Dept. of Marine, Earth and Atmospheric Sciences, North Carolina State University, Box 8208, Raleigh, NC 27695-8208.

Very little attention has been given to the formation, maintenance, and seasonal cycle of cloudiness in this region. The seasonal variation is important because clouds strongly affect the earth's radiation budget through changes in radiative fluxes. In order to understand the processes responsible for cloudiness in this region, a climatological description of the geographical and seasonal distribution would be useful. This study will therefore investigate the seasonal and geographical variations in cloudiness over the GSL.

The formation of clouds have been related to meteorological parameters such as atmospheric humidity. This information has, in turn, been used by numerical models to approximate fractional cloudiness in the atmosphere. Currently, however, large-scale numerical models of the atmosphere approximate the heterogeneous, subgrid-scale nature of cloudiness by assuming only a fraction of each grid area is occupied by clouds. This cloud cover fraction is used to apportion a significantly different cloud forcing into a "grid-averaged" forcing that contains a mixture of clear and cloudy regions. Most numerical weather prediction models assume the fractional cloud coverage is determined by the "grid-averaged" relative humidity, stability, or resolvable-scale vertical motions (Slingo 1980). In an attempt to evaluate how well humidity is related to cloudiness in numerical models, a comparison of satellite-derived cloudiness with relative humidity obtained from the National Meteorological Center's (NMC) global analyses is performed.

In this study we use a subset of the satellite-derived cloud dataset produced at the University of Wisconsin by Wylie and Menzel (1989) and Menzel et al. (1992). The Wylie–Menzel climatology (here after called W–M) was directed at mid- and upper-tropospheric clouds, particularly transmissive clouds over the continental United States. This research will use the GSL subset of the W–M climatology to evaluate cloud variations and to show the relationship to observed SST. In addition to reporting on mid- and upper-tropospheric clouds, an analysis of lower-tropospheric clouds is included.

The technique used to derive the W–M climatology is the CO_2 slicing technique. The CO_2 technique takes advantage of the differing partial CO_2 absorption in three of the infrared (IR) channels, with each channel sensitive to a different level in the atmosphere. Low clouds (those below 650 mb) are also included in the W–M climatology, but are derived directly from the 11-μm window channel. Also included in the dataset are cloud effective emissivities (also known as effective cloud amount), that are calculated from IR window channel observations. This information is valuable in discriminating opaque clouds from transmissive clouds. For a complete discussion on the cloud-retrieval techniques, the reader is referred to the references cited above. In addition, an extensive discussion on errors is given in these papers.

The motivation for using this dataset in describing cloudiness over the GSL is threefold. 1) The W–M dataset contains nearly seven years of continuous information in this region at approximately 6-h intervals (0000, 0600, 1200, and 1800 UTC). 2) The field of view (FOV) is approximately 10 km × 30 km or 300 km^2, and cloud heights are derived at 50-mb intervals. This is superior to other cloud climatologies, such as the International Satellite Cloud Climatology Project (ISCCP) dataset, which is also available for this region but at 250-km resolution (Rossow and Schiffer 1991). The use of a relatively high-resolution cloud dataset is essential for any cloud study in the GSL due to the large observed seasonal variability in cloudiness. 3) The VAS CO_2 cloud-top height and emissivity assignments have been found to be reliable in most cloud types, including thin cirrus clouds where other techniques have been inconsistent (Wylie and Menzel 1989). Finally, we attempt to further validate this dataset by making direct comparisons to National Weather Service (NWS) surface observations of cloudiness.

2. Mean statistics

A summary of all cloud observations obtained from December 1985 through November 1993 (not including the period March 1986–May 1987) is shown in Table 1. Approximately four million observations were processed during this period. Because of the large sample size and the relative accuracy of the CO_2 slicing technique, entries in Table 1 and for all other reports of cloud occurrence frequencies are valid within 1% (Menzel et al. 1992). Cloud-top pressure (CTP) evaluations are subdivided into four categories. Those less than 400 mb represent high cloudiness, and those between 400 mb and 650 mb are defined as midlevel clouds. CTPs greater than 650 mb but less than 1000 mb include the correct identification of low opaque clouds, errors from not resolving thin transmissive clouds, evaluation of ground as low cloud, and the incorrect identification of broken or scattered low clouds as opaque cloud. For simplicity this category will be referred to as "low cloud." Clear sky conditions are labeled as such. An "X" has been used to indicate where

TABLE 1. Cloud observations (frequency of occurrence; %) (December 1985–February 1986, June 1987–November 1993) for the Gulf Stream locale 31°–38°N, 81°–66°W. An "X" denotes where no additional cloud information is possible.

Cloud-top pressure (CTP) (mb)	Effective cloud amount			
	0.0–0.33	0.34–0.65	0.66–0.95	0.96–1.00
CTP < 400	6.3	8.2	11.7	5.0
400 ≤ CTP < 650	0.5	2.2	2.5	5.4
650 ≤ CTP < 1000	X	X	X	32.3
Clear sky conditions	25.5	X	X	X

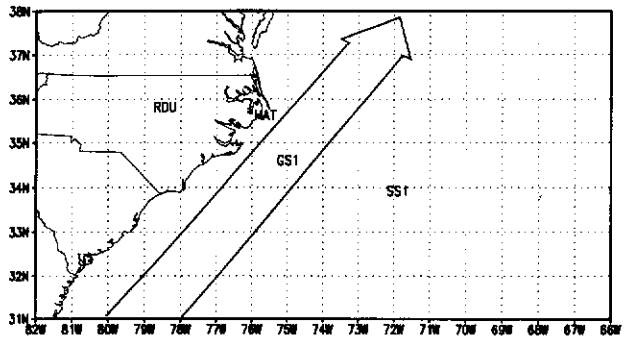

FIG. 1. Geographical coverage of the Gulf Stream locale. The large arrow represents the mean position of the Gulf Stream. The arrow separates the Gulf Stream from the shelf waters on the landward side from the Sargasso Sea on the seaward side. The symbols RDU, HAT, GS1, and SS1 represent the locations of Raleigh, North Carolina; Cape Haterras, North Carolina; the Gulf Stream; and the Sargasso Sea, respectively.

the satellite does not provide additional information. The effective cloud amounts (ECA) are subdivided into four categories shown in each column of Table 1. The right column contains the opaque or nearly opaque observations. Those ECA greater than 0.95 are considered to be opaque clouds since cloud-top heights derived from the CO_2 slicing algorithm are very close to heights derived from the IR window channel. The remaining three columns separate the cloud reports by ECA ranging from thin high and midlevel ECA in column 1 to thick high and midlevel ECA in column 3. An ECA for an opaque overcast cloud should be nearly 1.0 and should be zero for clear skies. An overcast cloud layer with an ECA significantly less than 100% indicates that the layer is thin, since some radiation passes through the clouds. The ECA that distinguishes between thin and opaque clouds for broken sky conditions will, in general, be lower than for overcast conditions (Schreiner et al. 1993).

Table 1 indicates that high clouds are found 31.2% of the time (sum of row 1), midlevel clouds are identified 10.6% of the time (sum of row 2), and low clouds are found 32.3% of the time. The remaining observations are identified as clear sky, which are observed 25.5% of the time. Thus, the algorithm identifies clouds 74% of the time. Furthermore, of the total amount of high and midlevel clouds detected by satellite, approximately 31% are determined to be semitransparent to terrestrial radiation. This estimate is similar to observations made by Wylie and Menzel (1989), who found semitransparent clouds one-third of the time over most of North America.

The GSL covers an area of 1.7 million square kilometers. This area is made up of mountainous, piedmont, and coastal plain terrain. Over water lies the cool shelf waters, the Gulf Stream, and the Sargasso Sea. Figure 1 shows the geographical area that defines the GSL. At any given time, but particularly in cold-air advection situations, cloudiness may vary greatly in these areas. Satellite cloudiness for four specific locations are presented to show differences in cloud frequency as a function of season. Satellite cloudiness is obtained for Raleigh, North Carolina (denoted as RDU), Cape Hatteras, North Carolina (denoted as HAT), the Gulf Stream (denoted as GS1), and the Sargasso Sea (denoted as SS1). The average station spacing is approximately 250 km (refer to Fig. 1). Cloud statistics are computed for an area within a 50-km radius of each station. These statistics are summarized for the 81-month period in terms of the three cloud-height categories and clear sky conditions.

Table 2 shows the 81-month cloud summary for the four locations. High- and midlevel clouds (CTP < 650 mb) are identified over 40% of the time for each of the locations. A slight preference for high clouds over water and midlevel clouds over land is seen in the summary. Low clouds are found more often over RDU and SS1 (34.0% and 32.6% of the time, respectively) and less often over GS1 (24.4%). Clear sky observations are found least often over RDU and SS1 and most often over HAT and GS1. Satellite observations of low opaque clouds are more prone to error over land than over water due to the erroneous identification of clear sky as low cloud. This occurs most often in the early morning hours during the cold months when strong nocturnal inversions exist. The result is the development of stable boundary layers where very little mixing occurs (Mahrt 1985). This is not the case over a marine boundary layer at night. Since the ocean temperature has a small diurnal variation and surface sensible and latent heat fluxes remain high, the marine boundary layer remains well mixed. Therefore, it is believed that satellite-derived low clouds over a MBL are more reliable than those found over a SBL.

The seasonal variation in cloudiness for each location is also investigated. Winter is defined as December, January, and February (DJF); spring as March, April, and May (MAM); summer as June, July, and August (JJA); and fall as September, October, and November (SON). The winter and spring months cover six years of the W–M climatology, while the summer and fall

TABLE 2. Frequency of cloudiness (%) (December 1985–February 1986, June 1987–November 1993) for Raleigh, North Carolina (RDU); Cape Hatteras, North Carolina (HAT); the Gulf Stream (GS1); and the Sargasso Sea (SS1). Also shown are the latitudes and longitudes for each location. Refer to Fig. 1 for the geographical location of these sites.

			Cloud height			
	Lat (°N)	Long (°W)	High	Middle	Low	Clear sky
RDU	35.8	78.8	31.0	12.1	34.0	22.9
HAT	35.3	75.5	32.0	10.0	30.2	27.8
GS1	34.5	75.0	32.5	10.3	24.4	32.8
SS1	34.0	72.0	32.4	10.0	32.6	25.0

months include seven years of data. The frequency of occurrence of high plus midlevel clouds are shown for each location and season in Fig. 2a. Similarly, low clouds, clear sky conditions, transparent clouds, and opaque clouds are shown in Figs. 2b–e, respectively. During winter, total cloudiness is found most frequently at SS1 (82%), while it is found least frequently at GS1 (68%). The 14% difference is found over a 300-km distance and is attributed to the higher occurrence of low cloud at SS1 (Fig. 2c). During the advection of cold dry continental air (typically 5°C) over the warmer waters of GS1 (typically 25°C) and SS1 (typ-

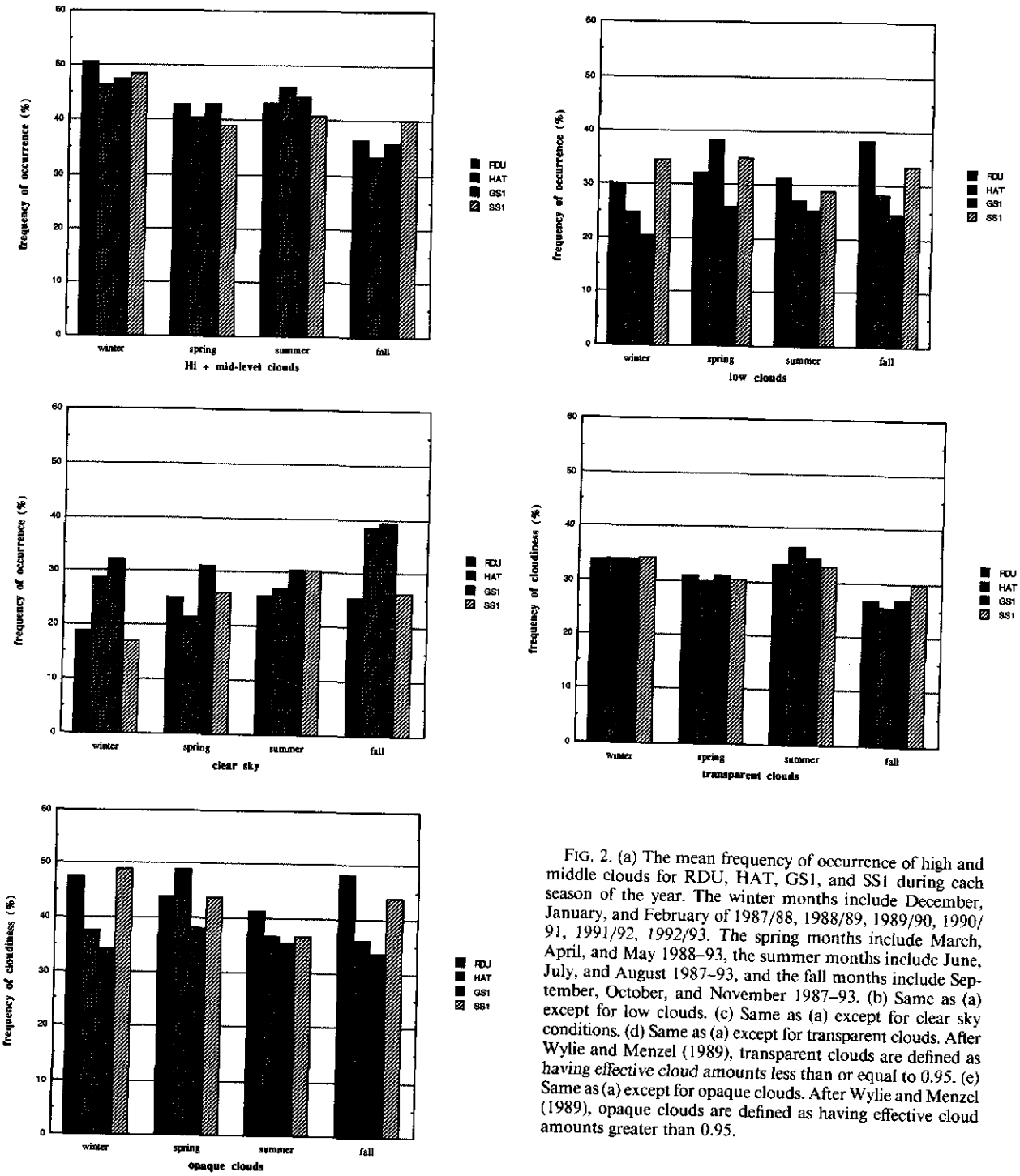

FIG. 2. (a) The mean frequency of occurrence of high and middle clouds for RDU, HAT, GS1, and SS1 during each season of the year. The winter months include December, January, and February of 1987/88, 1988/89, 1989/90, 1990/91, 1991/92, 1992/93. The spring months include March, April, and May 1988–93, the summer months include June, July, and August 1987–93, and the fall months include September, October, and November 1987–93. (b) Same as (a) except for low clouds. (c) Same as (a) except for clear sky conditions. (d) Same as (a) except for transparent clouds. After Wylie and Menzel (1989), transparent clouds are defined as having effective cloud amounts less than or equal to 0.95. (e) Same as (a) except for opaque clouds. After Wylie and Menzel (1989), opaque clouds are defined as having effective cloud amounts greater than 0.95.

ically 23°C), the thermodynamic characteristics of the air mass begin to change. As the air moves over GS1, large sensible and latent heat fluxes allow the convective MBL to grow rapidly (Wayland and Raman 1989). Eventually the air mass becomes saturated and unstable enough to support the development of stratocumulus clouds that align themselves along the wind trajectories. According to satellite estimates, the lower atmosphere on average is more conducive to clouds at SS1 than GS1, particularly during cold-air advection. This may vary greatly, however, depending on the actual intensity of the cold-air advection as well as the exact wind direction. Under extreme cold-air advection (air temperature less than −3°C) and strong surface winds, clouds may form between HAT and GS1 depending on the exact location of the Gulf Stream with respect to shore (Vukovich et al. 1991). While total cloudiness at RDU is identified by the technique 81% of the time, obvious errors associated with the spurious identification of clear sky as low cloud indicates an overestimate of total cloudiness. Errors in low-cloud retrievals at HAT are probably found less often due to the relatively warm waters surrounding this location. The occurrence of transparent clouds does not show any variation between the four sites (Fig. 2d). Opaque cloudiness, conversely, shows a maximum over both RDU and SS1 (Fig. 2e).

During the spring, the amount of high- and midlevel clouds identified at each location decreases approximately 7% compared with winter (Fig. 2a). The occurrence of low cloud rises, however, at all sites (Fig. 2b). The increase in the frequency of low cloud may be partly associated with the reduction in high- and midlevel cloudiness. When high- and midlevel clouds are present, the satellite is unable to detect low clouds. Additionally, boundary layer heating, which increases during the spring, results in an increase in low clouds, particularly over land. Over GS1, cold-air advection occurs less frequently and is much weaker. This tends to reduce surface fluxes as the surface-layer air is warmer and consequently the air–sea temperature difference is reduced. Mesoscale convergence zones, however, are often induced by gradients in SST along the west wall of the Gulf Stream. These mesoscale convergence zones can condition the atmosphere to support cloudiness. As in winter, transparent cloudiness is found uniformly between the four sites (32%). Opaque clouds in spring are found more often at HAT and GS1 compared to winter. A reduction in opaque cloudiness is identified at SS1 and RDU.

The summer months are characterized by little overall change in the occurrence of high- and midlevel clouds (Fig. 2a). An increase in occurrence of transparent cloudiness at all four sites is reported, however. The majority of the clouds identified as transparent are also found to be high clouds. It is believed that high transparent clouds are related to the occurrence of convection over land. Over GS1, cloudiness is identified slightly more often during summer compared to winter. Over SS1, cloudiness is identified 16% less often than during winter. The decrease observed at this location is associated with the overall increase in stability of the atmosphere. The increase in stability is the result of a dominant area of subtropical high pressure that produces large-scale subsidence, thus inhibiting widespread cloud growth (Bunker 1976). Interestingly, clouds identified by this technique at SS1 tend to be more transparent (Fig. 2d). In these situations, the VAS may be detecting high cirrus anvils that are observed to advect over this region from land during periods of convection. Indeed, Bunker (1976) reports that the prevailing winds during summer are southwesterly over the GSL, which supports this theory.

During the fall season, high- and midlevel cloudiness are identified less than 40% of the time at all sites except SS1 (Fig. 2a). Low clouds, however, are observed more often at RDU and SS1 while less often at HAT and GS1. Except for SS1, transparent clouds at RDU, HAT, and GS1 are observed approximately as often. Opaque cloudiness is identified nearly 50% of the time at RDU and approximately 45% at SS1 (Fig. 2e). The majority of opaque cloudiness identified at RDU is low (650–1000 mb). Low opaque cloudiness is less meaningful at this site because of the uncertainties of the algorithm in reliably separating low cloud from ground during night.

To better validate VAS-derived cloudiness, cloud frequencies are compared with surface observations over land. Surface observations of cloudiness reported by NWS observers at RDU and HAT are available between 1985 and 1992 from the National Climatic Data Center (NCDC) archives. The surface estimates of cloudiness are limited to daytime (sunrise to sunset) observations and contain no information on cloud height. Estimates of the mean frequency of cloudiness (FOC) are compiled for each season during this period. The VAS cloud heights are truncated to include only those observations between sunrise and sunset. The results are summarized in Table 3. VAS estimates of cloud frequency at RDU agree well with surface esti-

TABLE 3. Comparisons of VAS-derived frequency of cloudiness (%) and surface observations of cloudiness during daytime at RDU and HAT (December 1985–February 1986, June 1987–December 1992). Also included is the satellite–surface observation difference. A positive difference indicates an overestimate by the satellite retrieval technique.

	RDU			HAT		
Season	Satellite	Surface	Difference	Satellite	Surface	Difference
Winter	69.8	68.7	+1.1	75.9	72.9	+3.0
Spring	66.8	70.2	−3.4	74.9	69.3	+5.6
Summer	72.3	75.7	−3.4	78.5	76.4	+2.1
Fall	60.7	62.7	−2.0	67.3	66.0	+1.3
Total	67.4	69.3	−1.9	74.2	71.2	+3.1

mates. During winter, VAS slightly overestimates the FOC, while during spring, summer, and fall the technique underestimates the cloud frequency. For the entire time period, the technique tended to underestimate FOC but only by 2.0%. At HAT, agreement between the satellite observations and surface observations are slightly worse. The CO_2 technique overestimates cloudiness in all four seasons (5.6% in spring). Overall, the satellite detects cloudiness 3.1% more often than is found in the surface reports. The over detection of clouds at the Cape Hatteras coastal station may arise from coastal errors in the NMC temperature analysis used to determine cloud heights or from low marine clouds under reported by the Haterras observers. Although differences between estimated surface and satellite cloudiness are relatively small, errors may arise from the following. 1) Observations are made every hour by the observer and are averaged for each day. The satellite derives cloud information at 6-h intervals. 2) The FOV of the satellite is slightly different than the FOV of the observer, which is dependent on the visibility at the time of observation. 3) Additionally, satellites generally provide a better view of high clouds, while surface observers provide more reliable information on low-level cloudiness.

3. Geographical coverage, seasonal cycles, and relationship to sea surface temperatures

The geographical and seasonal distribution of VAS-derived total cloudiness is summarized in Figs. 3a–d. There are six winter and spring seasons and seven summer and fall seasons included in this summary. The mean SST for the same time period is included to show its relationship to cloud frequencies. The Miami multichannel sea surface temperature (MCSST) 18-km resolution dataset is used to describe the sea surface temperature (Smith 1992). December, January, and February (DJF) are characterized by the large gradients in both observed cloudiness and SST. Cloudiness along the coast is identified least often with the absolute minimum (<60%) found in a region near the core of the Gulf Stream (22°C). To the east of this area observed cloudiness increases in frequency rapidly. The large gradient in cloudiness along the land–sea interface is partly associated with the overestimate of cloudiness over land. This overestimate accounts for approximately 1%–5% of the observations; thus the data show a land–sea difference in spite of the documented satellite-detection error over land. SST gradients along the coastline typically range from 5° to 10°C (100 km)$^{-1}$ during winter. As shown in Fig. 3a, the frequency of cloudiness along these SST gradients shows a decrease in cloudiness from the coastline to the Gulf Stream front. This decrease may be associated with airmass modification processes during northwesterly flow (i.e., cold-air outbreaks). During winter, when the advection of cold dry continental air over the Gulf Stream dominates, the rapid influx of moisture and heat at the surface in response to the large surface sensible and latent heat fluxes produces a decrease in the height of the lifted condensation level (Vukovich et al. 1991). In their study, the authors report that at a certain point offshore, the average height of the marine boundary layer and the average height of the lifted condensation level intersect. It is at this point where convective elements within the boundary layer may produce cloudiness. According to seven years of VAS data, this intersection may lie just east of the Gulf Stream core. Analyses of sounding data will be needed, however, to prove this hypothesis. This is an important finding since typically between 15 and 20 cold-air outbreaks are observed in the GSL during winter, with approximately five of these episodes classified as intense (surface air temperature less than 0°C) (Wayland and Raman 1989). The duration of these events has been shown to last on the order of 1–2 days.

An increase in cloudiness to the east of the Gulf Stream is observed. According to Bunker (1976), prevailing winds in the GSL during winter are northwesterly with mean total surface fluxes exceeding 600 W m^{-2}. This supports the satellite observations of increasing cloudiness seaward of the Gulf Stream core. SST gradients in this area of the GSL are much weaker, however, and vary no more than 1°C (200 km)$^{-1}$. In these areas, cloudiness is identified more than 75% of the time. This maximum is probably associated with departing midlatitude cyclones that develop and intensify in this region (Colucci 1976). Typically, during periods of rapid cyclogenesis, the associated cloud shield expands and covers the entire GSL (Fig. 4). Cione et al. (1993) reports that cyclogenesis within the GSL occurs 10 times per winter season and lasts on the order of 2–4 days.

An increase in SST, a decrease in SST gradients, and an increase in observed cloudiness are all found during the spring months over the Gulf Stream (Fig. 3b). However, maximum observed cloudiness is found to the west of the Gulf Stream off the coasts of Virginia and North Carolina. This area is associated with much cooler SSTs (14°C) compared with those found over the Gulf Stream core (21°C). The majority of cloudiness is also identified as low and midlevel opaque cloud. Similar observations are reported in Bunker (1976) who found that this region was dominated by stratocumulus cloudiness during April and May. Over the southern portion of the Gulf Stream, cloudiness is observed least often (<70%). More clouds, however, are observed farther north over the Gulf Stream. Also, cloudiness well east of the Gulf Stream is found less often in spring compared with winter. This decrease is associated with the northward advancement of the midlatitude storm track. An interesting feature is observed during spring as the cloudiness contours closely align themselves with the shape of the Gulf Stream.

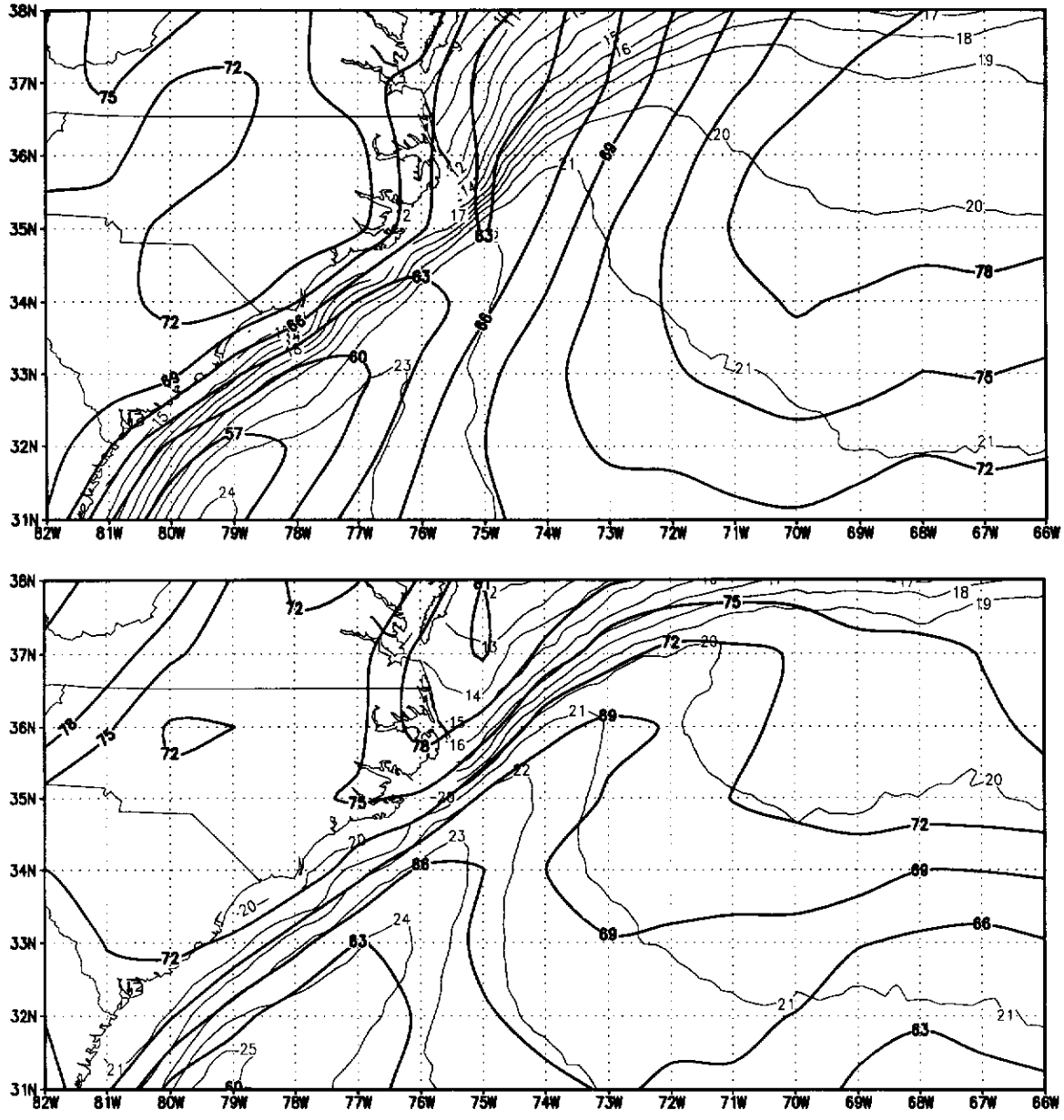

FIG. 3. (a) The mean frequency of occurrence (%) of total cloudiness (heavy lines) and sea surface temperature (°C) (thin lines) during winter 1987/88, 1988/89, 1989/90, 1990/91, 1991/92, 1992/93. (b) Same as (a) except for spring 1988–93.

Also, stronger gradients in cloudiness are associated with strong gradients in SST.

SSTs in summer are found to range from 24° to 27°C in the GSL with VAS-derived total cloudiness ranging from 60% to 63% over water (Fig. 3c). Except over the mountains, very little geographical variation is present. As alluded to earlier, air in this region is subsiding slightly under the influence of subtropical high pressure; thus, widespread convective cloudiness is inhibited. Low clouds during summers are found approximately 20% of the time. Unlike winter when stratocumulus type clouds are present, low clouds during summer tend to be more scattered in nature and confined to the lower troposphere. A decrease in opaque cloud occurrence in the summer is also found. This decrease is probably associated with the northward movement of the subtropical high pressure system during summer. Hahn et al. (1982) found a decrease in stratus clouds in summer in this area, but they also noted an increase in cumulus clouds. A strong correlation between stratus clouds and lower-tropospheric stability is shown by Klein and Hartmann (1993). They found an increase in atmospheric stability is associated with an increase in stratus cloud amount. This may

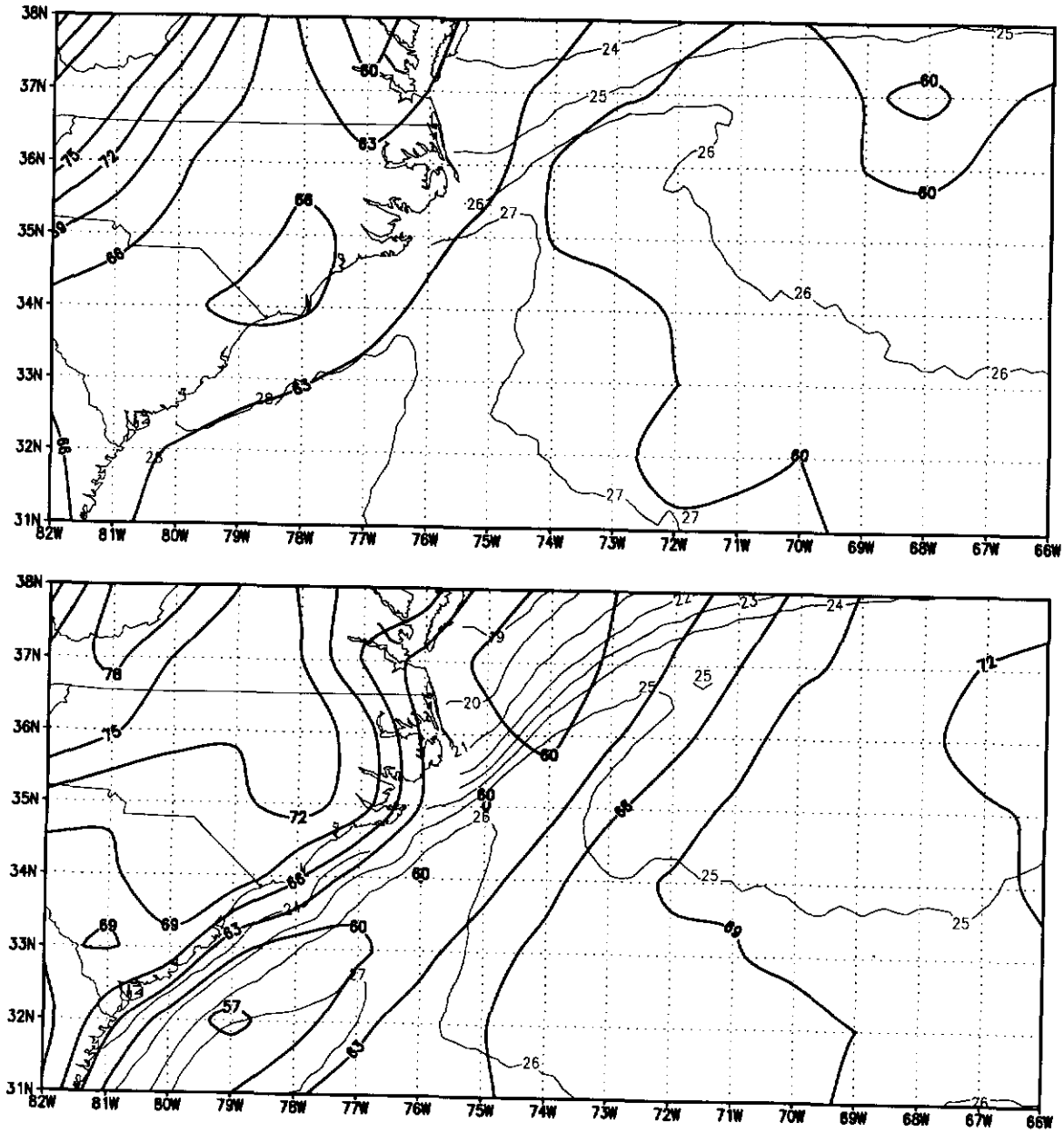

FIG. 3. (*Continued*) (c) Same as (a) except for summer 1987–93. (d) Same as (a) except for fall 1987–93.

help to explain the lack of stratus in the GSL during summer. High cloudiness is observed about 35% of the time in a tongue extending southwest to northeast over the Gulf Stream. This may be associated with the development of convection and the subsequent production of cirrus over the southeast states and the Gulf Stream. SST gradients increase again during fall as the shelf waters begin to cool (Fig. 3d). Additionally, cloudiness is detected least often over the shelf waters with an increasing trend seaward. Off the coast of Virginia, cloudiness is found greater than 60% of the time over the cooler waters to the northwest of the Gulf Stream (much like spring). The high occurrence of clouds (>70%) detected over land is overestimated by as much as 10% due to observations of ground being incorrectly identified as low cloud.

4. Comparisons with relative humidity analyses

Relative humidity (RH) fields used in this analysis are taken from NMC global analyses for the month of January 1991. These RH fields are available at 0000 and 1200 UTC. The levels available from the analysis include the 1000-, 850-, 700-, 500-, and 300-mb levels. The mean RH between 850 and 700 mb is used, however, to represent the level at which low

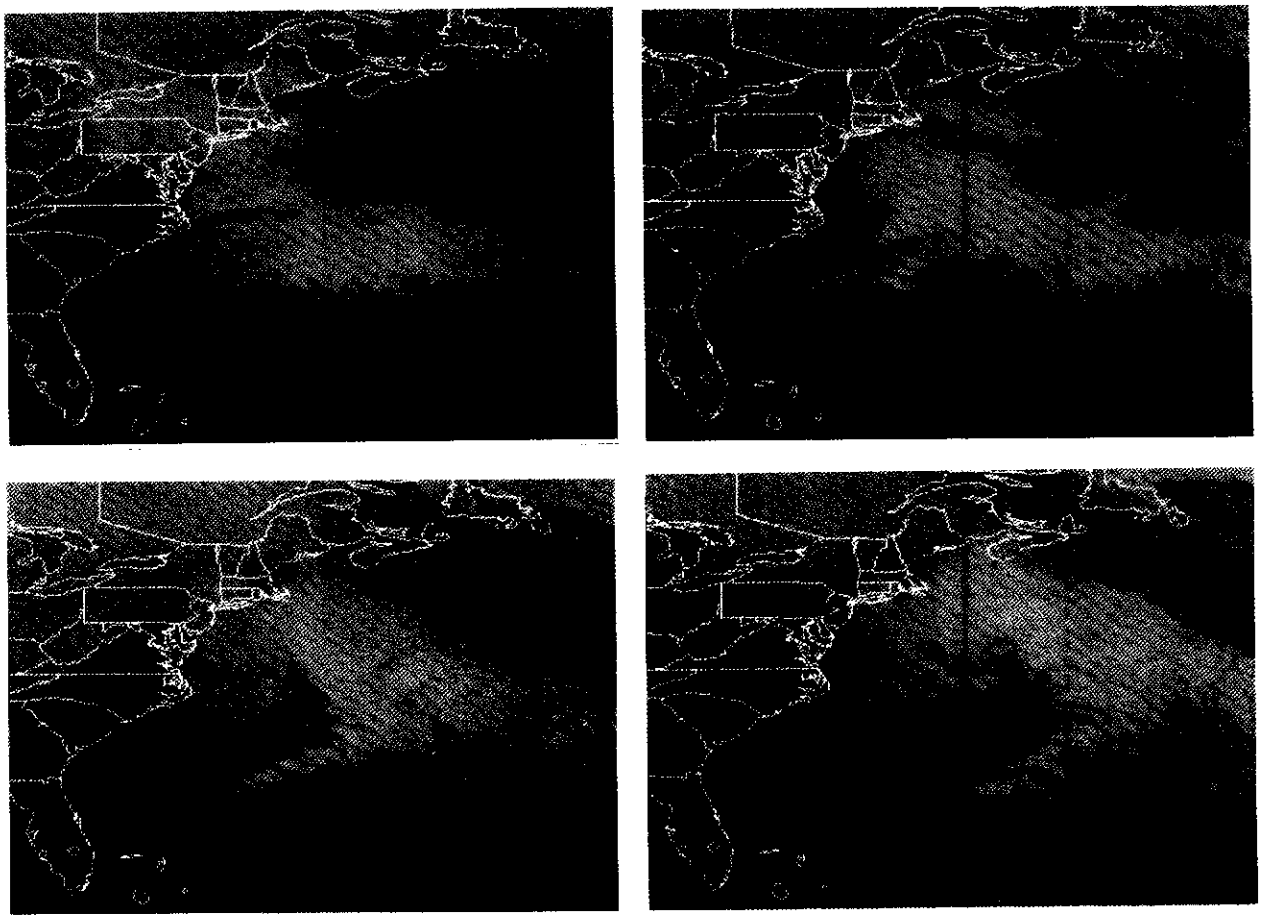

FIG. 4. GOES infrared images of an intensifying midlatitude cyclone over the Gulf Stream locale. The images are taken at 3-h intervals: 0000, 0300, 0600, and 0900 UTC 3 January 1989. The expansion of the cloud field is quite evident during the 9-h period. At 0600 and 0900 UTC, cloud streets are observed to the east of the Gulf Stream as cold advection takes place. A distinct cloud-free path is identified between the coastline and Gulf Stream core.

clouds may be found. The 300- and 500-mb RH represent levels at which high and middle clouds may occur, respectively. The horizontal resolution of the analyses is a coarse 2.5° × 2.5°. Therefore, in order to collocate the model analyses with the satellite data, a "composite" satellite report is derived for an area equal to that of the 2.5° × 2.5° global analysis. This is accomplished by determining the most frequently observed cloud height within each grid box. This cloud height is then used to represent the 2.5° × 2.5° area in the comparison. Within the GSL, there are three such 2.5° × 2.5° grid areas. In addition, the "composite" report is made at the closest time to the 0000 and 1200 UTC NMC analysis. For this analysis, VAS observations are available at 2350 and 1148 UTC. Due to poor vertical resolution of the NMC analyses, comparisons are limited to cloudiness detected at 300 and 500 mb and those detected between 850 and 700 mb.

Cloud heights derived from the CO_2 technique are cross correlated with the corresponding RH and summarized for each level (Fig. 5). Cloud reports are averaged in 25% increments for the 300-, 500-, and 850–700-mb levels. Approximately 155 observation pairs were made during this month; 300-mb clouds are found most often. As expected, the frequency of high clouds increases with increasing RH. Clouds at 300 mb, however, are associated with RH as low as 25%–50% (26% of 300-mb observations). No high clouds are identified at RH less than 25%. Only seven satellite–model pairs were identified for clouds at 500 mb. Of these seven, 57% are associated with RH between 51%–75% and only 15% are associated with RH > 76%. Clouds near 500 mb are found more often at RH between 26% and 50% than at RH > 76%. Clouds identified in the 850–700-mb layer are associated most often with RH > 76%. At lower RH, low clouds in the 850–700-mb layer are found less often. Interestingly, Fig. 5 shows that 16%–28% cloud occurrence occurs at humidities as low as 25%, in contrast to many parameterization that set zero could cover at humidities below 50%–80% (Walcek 1994).

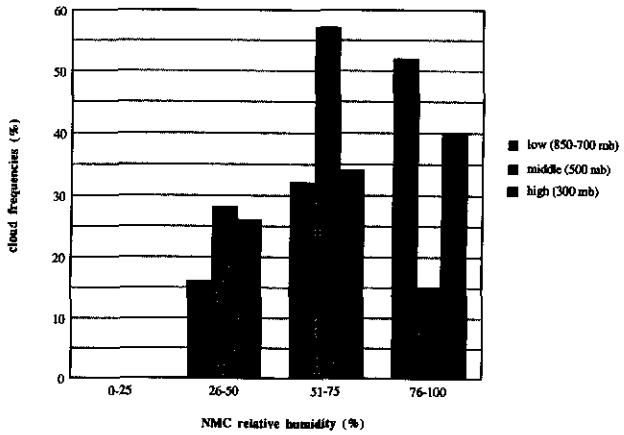

FIG. 5. VAS-derived high-, mid-, and low-cloud frequencies for January 1991 as a function of NMC analyses of relative humidity. Clouds at all levels are found at relative humidities as low as 26% but are more commonly found at humidities greater than 50%. No clouds are found at relative humidities below 25%.

The vertical resolution of the model analyses in this case is limited to three levels. Therefore, cloudiness at other levels is not considered. These results, although for a limited domain, a limited time period, and a coarse resolution, demonstrate that the FOC decreases as relative humidity falls below 100%. Although a "critical relative humidity" where cloud coverage is always zero cannot be determined, the probability of detecting cloudiness on this scale at RH < 25% is quite small.

5. Summary and conclusions

In the present study, the frequency of cloudiness over the GSL obtained from the Wylie–Menzel GOES VAS cloud climatology has been investigated. The purpose of the study was to investigate the seasonal variations of cloudiness in a region that has been shown to be highly baroclinic due to the proximity of the Gulf Stream to the United States east coast. In addition, the study has discussed possible relationships of cloudiness to the various meteorology of the region. The results obtained in this pilot exercise are both intriguing and encouraging. In this study, several important findings have emerged. Cloudiness is found as often as three-quarters of the time in the GSL. Mean cloudiness in the GSL, which was first thought to occur most often over the Gulf Stream core, is actually found less often. VAS observations of cloudiness over land and over the Sargasso Sea are found more often than over the Gulf Stream core. The maximum cloudiness is most often observed east of the Gulf Stream during the fall and winter. During summers, cloudiness is generally found less often as large-scale subsidence and greater atmospheric stability in the region inhibits large-scale convective cloud regimes. Over the Gulf Stream, localized cloudiness is observed to form in response to mesoscale convergence areas produced by gradients in sea surface temperature. In some instances, however, very small cloud elements may go undetected by VAS due to sensor resolution. Horizontal gradients in the frequency of cloudiness are also found to show remarkable similarity to sea surface temperature gradients. This was particularly evident during fall, winter, and spring. During summer, only small variations in sea surface temperature and cloudiness were found. Over land, observations from satellite were less reliable. VAS observations during daytime, however, compared well to surface reports of cloudiness. At RDU satellite observations tended to slightly underestimate surface observed cloudiness, while at HAT the cloud retrieval techniques overestimated cloudiness compared to those reported by the observer.

The frequency of cloudiness estimated from satellite was cross correlated with relative humidity from a large-scale numerical model. Results indicate that clouds were observed at relative humidities as low as 26%. Since moisture is poorly measured by rawinsondes, particularly in the upper atmosphere, it is not all surprising that clouds are found where the NMC analyses indicate low relative humidity. Typically, however, cloudiness was found in higher humidities regimes. This simple comparison has its limitations, in particular with regard to the coarse resolution of the model. Comparisons of satellite cloudiness and other related meteorological variables such as stabilities, vertical velocities, and wind shear are, however, being performed using NMC's step-coordinate eta model. Satellite-derived cloud parameters may be potentially useful in quantitative verification of moisture in numerical models. In turn, a better understanding of cloud-formation mechanisms may facilitate improvements and refinements in current condensation–cloud parameterization schemes.

There are some weaknesses in the satellite retrieval methods that have to be addressed before we can have sufficient confidence in the data to make quantitative comparisons with model simulations meaningful. For instance, since the VAS CO_2 slicing technique cannot be used to reliably identify low clouds, a simple threshold technique using the 11-μm window channel is used. When using the threshold technique, however, problems arise from errors in estimating the surface temperature during nocturnal cooling of the ground. In these situations, the threshold technique will falsely detect low clouds. This worry is less of a problem over marine boundary layers. The problem may be alleviated over land somewhat with the inclusion of available rawindsonde data, which can give information about the relative humidity of the supposed cloud layer. If the relative humidity does not satisfy some threshold, perhaps 90%, then the low cloud may be correctly classified as clear sky. Furthermore, the retrieval technique does not provide complete coverage of low broken

cloudiness (CTP > 650 mb). It is necessary to assume that only one cloud layer is present. Under strong dynamic conditions, multiple cloud layers are often present over the GSL. The VAS CO_2 slicing technique does provide excellent coverage of middle and high cloudiness. The coupling of both ground and satellite reports of cloudiness may be useful in providing more complete and accurate cloud coverage.

Acknowledgments. The authors wish to express their gratitude to Don Wylie of the Space Science and Engineering Center, University of Wisconsin—Madison, for graciously providing us with the VAS cloud height dataset. We also extend our thanks to the reviewers who provided us with helpful suggestions to improve the manuscript. This work was supported by the Department of Energy's Atmospheric Radiation Measurement program under Contract 091575-A-Q1 with Pacific Northwest Laboratories.

REFERENCES

Budyko, M. I., 1963: Guide to the atlas of the heat balance of the earth. U.S. Weather Bureau, WB/T0106, translated by I. A. Donehoo, U.S. Weather Bureau, Washington, DC.

Bunker, A. F., 1976: Computations of surface energy flux and annual air–sea interaction cycles of the North Atlantic Ocean. *Mon. Wea. Rev.*, **104,** 1122–1140.

Chang, S. W., R. J. Alliss, S. Raman, and J. J. Shi, 1993: SSM/I observations of ERICA IOP 4 marine cyclone: A comparison with in situ observations and model simulation. *Mon. Wea. Rev.*, **121,** 2452–2464.

Cione, J. J., S. Raman, and L. J. Pietrafesa, 1993: The effect of Gulf Stream–induced baroclinicity on U.S. East Coast winter cyclones. *Mon. Wea. Rev.*, **121,** 421–430.

Colucci, S. L., 1976: Winter cyclone frequencies over the eastern United States and adjacent western Atlantic, 1964–1973. *Bull. Amer. Meteor. Soc.*, **57,** 548–553.

Dirks, R., J. P. Kuettner, and J. Moore, 1988: Genesis of Atlantic Lows Experiment (GALE): An overview. *Bull. Amer. Meteor. Soc.*, **69,** 148–160.

Hahn, C. J., S. G. Warren, J. London, R. M. Chervin, and R. Jenne, 1982: Atlas of simultaneous occurrence of different cloud types over the ocean. NCAR Tech. Note, NCAR/TN-201+STR, 212 pp.

Holt, T., and S. Raman, 1990: Marine boundary-layer structure and circulation in the region of offshore redevelopment of a cyclone during GALE. *Mon. Wea. Rev.*, **118,** 392–410.

Huang, C. Y., and S. Raman, 1991: Numerical simulation of January 28 cold air outbreak during GALE. Part II: The mesoscale circulation and the marine boundary layer. *Bound.-Layer Meteor.*, **56,** 51–81.

Klein, S. A., and D. L. Hartmann, 1993: The seasonal cycle of low stratiform clouds. *J. Climate,* **6,** 1587–1606.

Mahrt, L., 1985: Vertical structure and turbulence in the very stable boundary layer. *J. Atmos. Sci.*, **42,** 2333–2349.

Menzel, W. P., D. P. Wylie, and K. I. Strabala, 1992: Seasonal and diurnal changes in cirrus clouds as seen in four years of observations with VAS. *J. Appl. Meteor.*, **31,** 370–385.

Raman, S., and A. J. Riordan, 1988: The Genesis of Atlantic Lows Experiment: The planetary boundary layer subprogram. *Bull. Amer. Meteor. Soc.*, **69,** 161–172.

——, ——, T. Holt, M. Stunder, and J. Hinman, 1986: Observations of the marine boundary layer thermal structure over the gulf stream during a cold-air outbreak. *J. Appl. Climate Meteor.*, **25,** 14–21.

Rossow, W. B., and R. A. Schiffer, 1991: International Satellite Cloud Climatology Project (ISCCP) data products. *Bull. Amer. Meteor. Soc.*, **72,** 2–20.

Schreiner, A. J., D. A. Unger, W. P. Menzel, G. P. Ellrod, K. I. Strabala, and J. L. Pellet, 1993: A comparison of ground and satellite observations of cloud cover. *Bull. Amer. Meteor. Soc.*, **74,** 1851–1861.

Slingo, J. M., 1980: A cloud parameterization scheme derived from GATE data for the use with a numerical model. *Quart. J. Roy. Meteor. Soc.*, **106,** 747–770.

Smith, E., 1992: *A User's Guide to the NOAA Advanced Very High Resolution Radiometer Multichannel Sea Surface Temperature Data Set.* California Institute of Technology, 1–20. [Available from the Physical Oceanography Active Archive Center, Jet Propulsion Laboratory, California Institute of Technology, Pasadena, CA.]

Vukovich, F. M., J. W. Dunn, and B. W. Crissman, 1991: Aspects of the evolution of the marine boundary layer during cold-air outbreaks off the southeast coast of the United States. *Mon. Wea. Rev.*, **119,** 2252–2279.

Walcek, C. J., 1994: Cloud cover and its relationship to relative humidity during a springtime midlatitude cyclone. *Mon. Wea. Rev.*, **122,** 1021–1035.

Wayland, R., and S. Raman, 1989: Mean and turbulent structure of a baroclinic marine boundary layer during the 28 January 1986 cold air outbreak (GALE 86). *Bound.-Layer. Meteor.*, **48,** 227–254.

Wylie, D. P., and W. P. Menzel, 1989: Two years of cloud cover statistics using VAS. *J. Climate,* **2,** 380–392.